

Article

The Impact of Temperature and Power Variation on the Optical, Wettability, and Anti-Icing Characteristics of AZO Coatings

Kamlesh V. Chauhan ¹, Sushant Rawal ^{2,*} , Nicky P. Patel ³  and Vandan Vyas ¹ 

¹ CHAMOS Matrusanstha Department of Mechanical Engineering, Chandubhai S. Patel Institute of Technology (CSPIT), Charotar University of Science and Technology (CHARUSAT), Changa 388421, Gujarat, India; kamleshchauhan.me@charusat.ac.in (K.V.C.); vandan.vv@gmail.com (V.V.)

² McMaster Manufacturing Research Institute (MMRI), Department of Mechanical Engineering, McMaster University, 1280 Main Street West, Hamilton, ON L8S4L7, Canada

³ Department of Mechanical Engineering, Ipcowala Institute of Engineering and Technology, Ipcowala Education Campus, Petlad-Khambhat Highway Rd., Dharmaj 388430, Gujarat, India; nicky_ptl@yahoo.co.in

* Correspondence: sushant@mcmaster.ca

Abstract: The structural, wettability, and optical characteristics of aluminum-doped zinc oxide (AZO) thin films were studied with the objective of understanding the impact of deposition power and deposition temperature. Thin films were deposited using a radio frequency (RF) magnetron sputtering technique. The power output of the RF was augmented from 200 to 260 W, and the temperature was increased from 50 to 200 °C, which led to the development of a (002) peak for zinc oxide. The study of film thickness was carried out using the Swanepoel envelope method from data obtained through the UV-Vis spectrum. An increase in surface roughness value was shown to be connected with fluctuations in temperature as well as increases in deposition power. The findings revealed that as deposition power and temperature increased, the value of optical transmittance decreased, ranging from 70% to 90% based on the deposition parameters within the range of wavelengths that extend from 300 to 800 nm. The wettability properties of the samples were studied, and the maximum contact angle achieved was 110°. A Peltier apparatus was utilised in order to investigate the anti-icing capabilities, which revealed that the icing process was slowed down 3.38-fold. This work extends the understanding of the hydrophobicity and anti-icing capabilities of AZO thin films, specifically increasing both attributes which provide feasible options for purposes requiring resistance to ice.

Keywords: thin films; structural; optical; wettability; aluminum zinc oxide



Citation: Chauhan, K.V.; Rawal, S.; Patel, N.P.; Vyas, V. The Impact of Temperature and Power Variation on the Optical, Wettability, and Anti-Icing Characteristics of AZO Coatings. *Crystals* **2024**, *14*, 368. <https://doi.org/10.3390/cryst14040368>

Academic Editor: Marco Bazzan

Received: 8 March 2024

Revised: 8 April 2024

Accepted: 12 April 2024

Published: 15 April 2024



Copyright: © 2024 by the authors. Licensee MDPI, Basel, Switzerland. This article is an open access article distributed under the terms and conditions of the Creative Commons Attribution (CC BY) license (<https://creativecommons.org/licenses/by/4.0/>).

1. Introduction

The use of coating technology is crucial for several aspects of our everyday tasks. An extensive assortment of coatings has been developed for application on a wide array of things, including consumer and textile goods, pharmaceutical industries, industrial equipment, automobiles, and architectural components [1–5]. The application of a thin film or coating as an outer layer has the potential to successfully protect, improve, or impose unique capabilities and qualities on bulk materials and a variety of surfaces [6]. An extensive range of environmental elements, including weather conditions, humidity levels, and ice, all of which have the potential to produce chemical reactions, fouling, corrosion, and structural damage, can be controlled by the application of coating technologies. These technologies have the capacity to limit the effect of these environmental factors [7–9]. The use of coating technologies has the ability to confer a number of diverse characteristics and functions upon substrates. These characteristics and functions include anti-microbial qualities, hydrophobicity, and anti-icing capabilities [10,11]. As a consequence of this, development of multifunctional films and innovations, as well as their investigation and design have garnered a significant amount of attention and effort due to the economic value of these materials and the high demand that has resulted from the vast variety of

uses the materials have. In order to generate coatings, a number of different techniques can be utilised. Some of those methods include sol–gel dip and spin coating, pulsed laser deposition, chemical vapor deposition, atomic layer deposition, and sputtering [12–17].

In recent years, a significant amount of research has been conducted in the field to develop transparent conducting oxide films that have minimal resistance yet substantial transparency in the visible spectrum; with such properties, TCO has been vastly used for multiple applications such as organic light-emitting diodes, liquid crystal display, and solar cells [18,19]. Various materials like aluminum, titanium oxide, and zinc oxide are being researched for the development of such films, and aluminum-doped ZnO (AZO) coatings that possess remarkable electro-optical characteristics are being considered as alternatives to indium tin oxide-like thin films. Ali et al. conducted a study to investigate the impact of boron–cobalt co-doping on the optical and frequency-dependent electrical characteristics of ZnO thin films. Their findings revealed that the doping process resulted in enhanced optical and frequency electrical properties. Consequently, these films exhibit promising potential as viable options for optoelectronic devices [20]. Lekoui et al. conducted a study in which they synthesised Ag-Mn co-doped ZnO thin films and investigated their impact on the structural, optical, and mechanical characteristics of the thin films. Co-doping enhanced the hardness while reducing the optical transparency. Additionally, it was shown that the energy band gap exhibits a drop during co-doping, with values consistently remaining below those of the pure ZnO sample [21]. ZnO thin films doped with Ga and Mg were developed by Tiwari and Sahay. The researchers demonstrated that the introduction of doping resulted in enhanced optical and electrical conductivity. Additionally, it was said that the films possessed essential attributes indicative of a promising material suitable for utilisation in optoelectronic applications [22]. The high energy band gap makes zinc oxide a viable alternative for applications in the near-UV and Vis spectral range. Superior properties like this can be used for obtaining advanced devices. The deposition of AZO can be performed using the sol–gel dip and spin coating, chemical vapor deposition, magnetron sputtering, spray pyrolysis technique, etc., with various doping elements [23–26]. As a result of its band energy being more than 3.37 eV, zinc oxide (ZnO) may be utilised in a wide variety of commercial products, including pigments, paints, rubber, glass, metals, and batteries [27–32].

The current trend in research on wettability properties has piqued the interest of many researchers. Wettability properties can be modified by developing precise chemical properties and morphological properties of any surface. The wettability properties of the surface can be altered between hydrophobic and hydrophilic depending upon the applications required.

In addition to oil refineries, the maritime sector, the aviation industry, the power transmission organisation, and infrastructure companies all face a significant challenge in the form of ice formation. In addition to causing disruptions in functioning and a decrease in production, it also poses significant economic as well as security concerns, which can have devastating effects. There has been a significant amount of work put out in order to address this significant yet difficult problem. Even though there are many different de-icing tactics that are utilised, they are restricted by a number of problems, including the contamination of the environment, the usage of heavy equipment, and the high consumption of electricity, in addition to the requirement of consistent reapplication. There is a promising alternative technique known as surface modification that has the potential to simplify the de-icing operations that are already in place. It does this by minimising or avoiding the buildup of ice and by facilitating the detachment of ice that has already collected. In spite of the fact that this tactic is favourable, it does have certain restrictions with regard to mechanical properties, surface roughness, and surface qualities and characteristics. As a result, the strategy that is expected to be the most successful in decreasing the formation of ice is now being discussed. By imitating the surface of the lotus leaf, a wide range of hydrophobic surfaces have the potential to be used for purposes such

as anti-rusting surfaces, anti-fogging surfaces, anti-wetting surfaces, and anti-ice adherence properties [33–37].

The study of wettability properties and optical properties is limited in the literature. The objective of this research is to investigate the ways in which the surface characteristics of AZO thin films may be influenced by variables such as the deposition power and the deposition temperature. This research is aimed at developing hydrophobic properties for the application of self-cleaning glass. The structural, optical, and wettability properties have been explored in this research.

2. Materials and Methods

A specially made vacuum chamber with dimensions of 16" in diameter \times 14" in height was used for the deposition of thin films. An RF magnetron sputtering system was used to deposit the AZO target material (ZnO/Al, 98:2 wt%), which was 99.99% pure, onto a Corning glass substrate. There was a gap of 50 mm between the substrate and the surface. A mass flow controller designed by Alicat, Tucson, AZ, USA, was used to maintain a constant flow rate of 10 sccm of inert gas (argon) and reactive gas (oxygen). The deposition procedure lasted 60 min, with a constant deposition pressure of 2.5 Pa. Various substrate temperatures (50 °C to 200 °C) and RF power levels (200 W, 220 W, 240 W, and 260 W) were used during film deposition. AZO coatings were developed by sputtering, and the parameters that were employed are listed in Table 1.

Table 1. Parameters for sputtering used in the deposition of thin films.

RF Power	200, 220, 240, and 260 W
Temperature	50, 150, 200, and 250 °C
Pressure	2.5 Pa
Sputtering time	60 min
Distance between surface and substrate	50 mm
Argon/oxygen flow	10:10 sccm

Using a Bruker D2 Phaser X-ray diffractometer, we were able to determine the structural characteristics of the films. Topographic examination of materials was performed using a Nanosurf easyscan 2 atomic force microscope. Ramehart's Model 290 contact angle measurement equipment was also used to examine the films' wettability capabilities. For determining the transparency of the films, a Shimadzu UV-3600 plus UV-Vis spectrophotometer was used.

3. Results and Discussion

Figure 1a depicts an X-ray diffraction graph of coatings that were formed at different deposition powers of 200, 220, 240, and 260 W at a substrate temperature of 50 °C. Figure 1b depicts the same graph with a deposition power of 200 W at substrate temperatures of 50, 100, 150, and 200 °C.

An analysis was conducted on the XRD patterns of an aluminum zinc oxide thin film that had been formed at a substrate temperature of 50 °C and a power of 200 W, and a weak peak of (002) was observed (JCPDS reference card number-36-1451). The peak with the highest intensity was obtained at a power of 260 W, which shows that with the rise in power, the peak of the films becomes more prominent. Patel et al. (2022) observed a similarity in the (002) ZnO peak pattern. The peak of (002) ZnO had a low intensity at 170 W but improved as the power was elevated [38]. P. Misra et al. (2017) identified the same pattern of the (002) ZnO peak. As sputtered atoms become more intense as they approach the substrate, the impact of the high-energy electron bombardment on the developing coating grows [39]. The atoms that are being deposited on the substrate receive thermal energy from these two components, which enables them to move more freely and enhances the crystalline structure of the formed AZO layer.

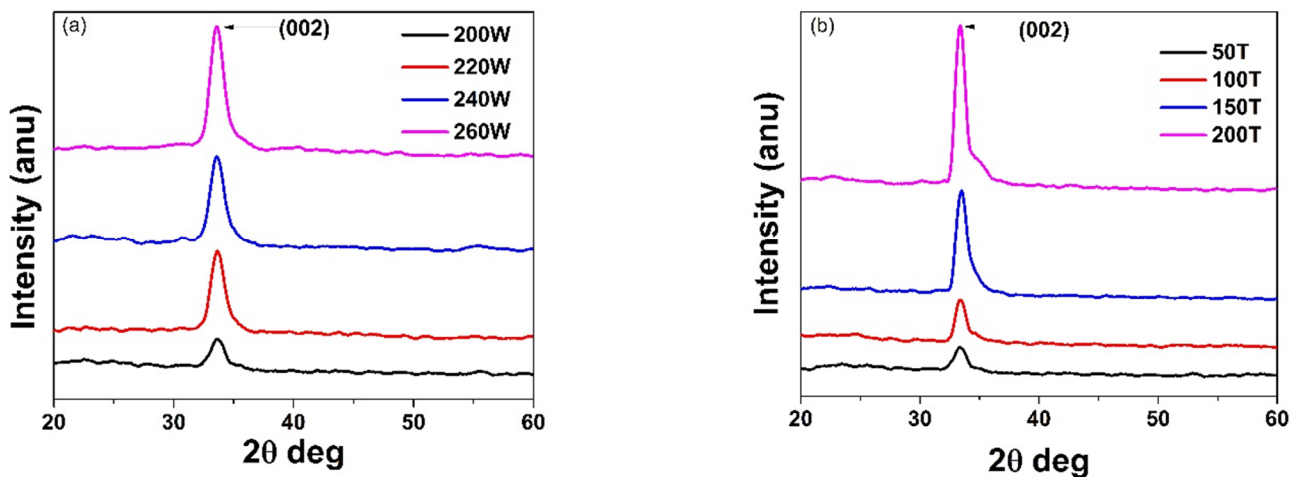


Figure 1. XRD patterns of thin film of aluminum zinc oxide prepared at various (a) sputtering powers and (b) temperatures.

A modest peak of (002) was observed at lower temperatures when the development of coatings was carried out at an RF power of 200 W and the substrate temperature was adjusted from 50 °C to 200 °C. This was the case when the substrate temperature was altered. When the temperature of the substrate was raised, it was observed that the intensity of the (002) peak improved as well. The results align with what has been found in previous studies [40–42]. The literature reveals that the AZO films exhibited the absence of aluminum phases in all samples, suggesting that the introduction of Al doping did not induce any structural phase transitions [43]. The measure of the average crystallite was ascertained by means of the Scherrer formula [44]. When the power varied from 200 to 260 W, the mean size of the crystallite grew from 22.80 to 26.23 nm. In a comparable vein, when the temperature was varied from 50 to 200 °C, the mean crystallite size improved from 6.20 to 18.41 nm.

In the generation of a hydrophobic surface, the surface must contain nanotextures and microtextures [45]. Wenzel and Cassie-Baxter developed two mathematical models that represent the connections between the amount of roughness and the contact angle, as shown in Equation (1) [46]. If the surface roughness increases, the value of the contact angle will increase as well. Conversely, if the nanostructure and microstructure of the surface decrease, the value of the contact angle continues to drop.

$$\cos\theta = A\cos\theta' \quad (1)$$

A = roughness factor;

θ = contact angle of water;

θ' = water contact angle distinguished based on interfacial energy.

Hydrophilic surfaces are those with values of θ less than 90°, while hydrophobic surfaces have values of θ greater than 90°.

An atomic force microscope was used to obtain images and determine the roughness of coatings deposited at varying temperatures and powers (Figure 2). It was concluded, on the basis of the observations, that a rise in surface roughness was caused by an increase in both the power of the deposition process and the temperature at which the coating was developed. While considering the deposition power, it was observed that with the elevation in deposition power from 200 to 260 W, the value of surface roughness increased from 23.2 nm to 54.6 nm, as shown in Figure 2a. This demonstrates that the bombardment exerted on the surface leads to a decrease in surface smoothness with higher sputtering power [38]. The value of surface roughness increased from 31.4 to 54.6 nm with an increase in deposition temperature, as shown in Figure 2b, which can be validated using the theory of recrystallisation due to an increase in temperature [47–49].

With the intent of determining the relationship between the contact angle and the roughness of the surface with regard to deposition power and temperature, the sessile drop technique was employed. Figure 3b displays the trend of an increase in contact angle from 86.8° at 50 °C to 109.7° at 200 °C of deposition temperature. It was observed that rise in deposition power from 200 to 260 W, the value of the contact angle varied between 107.1° and 110° while the roughness of the surface increased from 23.2 to 54.6 nm, as shown in Figure 3a. Thin films of aluminum zinc oxide showed an increase in the value of contact angle with an increase in surface roughness, which increased due to a change in the deposition parameter of the thin film. The surface energies of the developed coatings changed from 19.60 to 17.09 mJ/m² as the power increased from 200 to 260 W; similarly, the values of surface energy decreased from 31.22 to 18.19 mJ/m² as the temperature was increased from 50 to 200 °C. The decrease in surface energy has a favourable impact on the hydrophobicity of the coating.

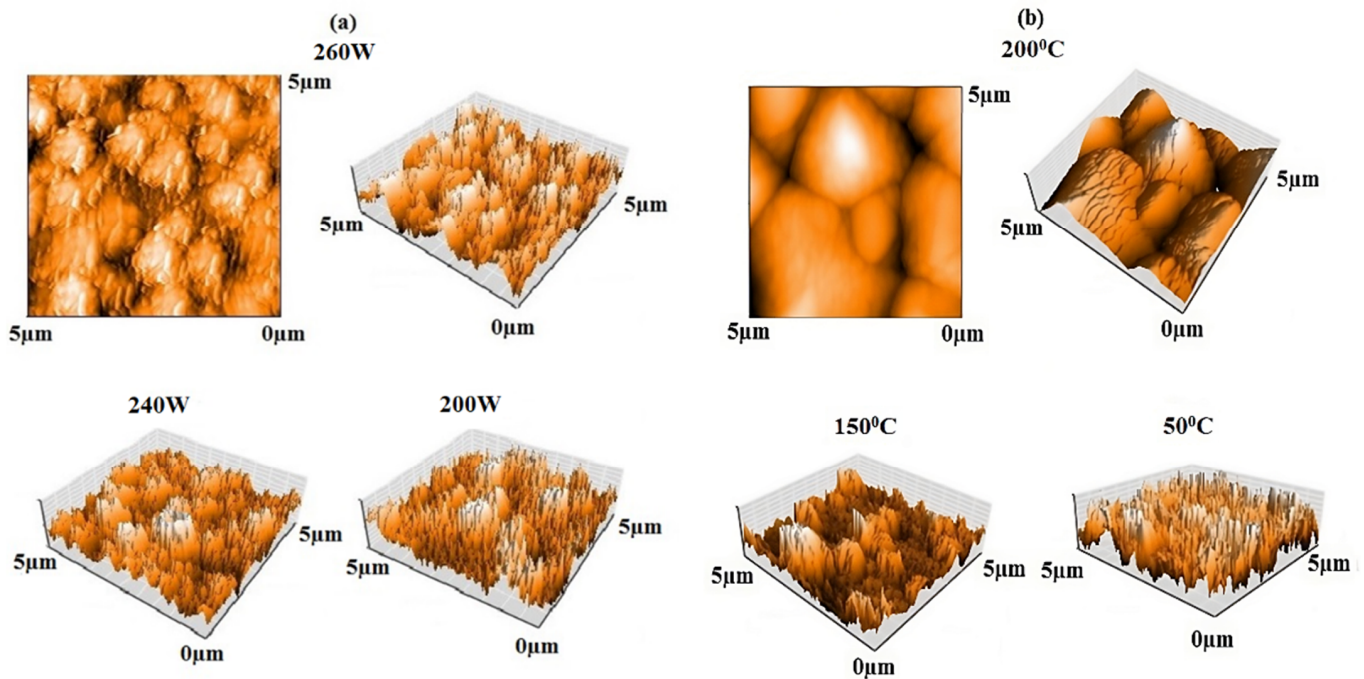


Figure 2. Atomic force microscope images of AZO thin film prepared at different (a) powers and (b) substrate temperatures.

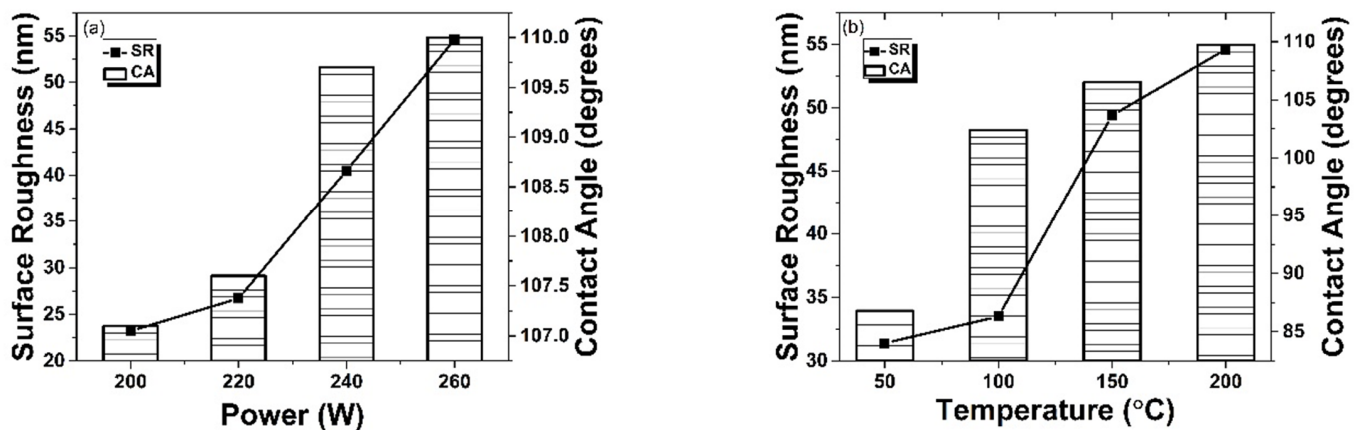


Figure 3. Relation between surface roughness and contact angle for thin films deposited at different (a) powers and (b) temperatures.

Consistent with what was found in the referenced literature, increasing the surface roughness improved the contact angle [50,51]. Furthermore, differences in temperature and RF power of formed thin films are connected with the composition of chemicals of the coatings when they are developed. The rate at which atoms may be retrieved from the sputtering chamber is a critical factor in determining the formation of AZO films [38]. Additionally, Ahmad et al. observed that the hydrophilic properties of a material may be tailored by several methods. This can be achieved by applying a molecular layer of a new material that is more hydrophilic than the original substrate or by altering the surface chemistry of the substrate [52].

The icing properties of the films made under different sputtering settings were studied with a Peltier cooler set up at a temperature of $-15\text{ }^{\circ}\text{C}$. Comparing treated and untreated Corning glass specimens of coatings showed that the coating caused a postponement in the icing process. Thin films formed at different substrate temperatures and powers show a rise in the icing time delay, as shown in Table 2.

Table 2. Wettability and anti-icing characteristics of coatings produced under different sputtering circumstances.

Sputtering Details	200 W	220 W	240 W	260 W	50 °C	100 °C	150 °C	200 °C
Water Contact Angle (°)	107.1	107.6	109	110	86.8	102.4	106.5	109.7
Time Delay (folds/times)	2.60	2.71	3.15	3.38	1.2	2.01	2.50	3.22

It was found that coatings that were synthesised at a power level of 260 W RF had an enormous time lag for ice formation, a delay that was 3.38 times greater than that for the specimens that were not treated. It was discovered that the formation of ice was slowed down significantly while considering the fact that the hydrophobic nature of the coatings improved from 107.1 to 110° in response to a shift in the power. A similar delay in the generation of ice was recorded for films that were created at a variety of temperatures. This delay was equal according to the findings. It took 3.22 times longer for films that were coated at a temperature of $200\text{ }^{\circ}\text{C}$ to generate ice on the surface when compared to a substrate that was not coated. According to the findings of recent scientific investigations, there appears to be a direct relationship between the ability of ice repellency and the ability of water repellency. Surface roughness is another key component that raises the water contact angle on surfaces, which progressively enhances the anti-icing capabilities of thin films. Materials with a low surface energy are one of the two primary variables that improve hydrophobic and anti-icing qualities. The second main factor is surface roughness.

S. Noormohammed and D. Sarkar conducted a study to determine the impact that water-resistant coatings have on the adherence and growth of ice. The findings of this study were published in one of their papers. According to their findings, possibilities for icephobic surfaces that are acceptable include hydrophobic surfaces that are governed by geometry and chemistry. A further finding that they noticed was that the strength of the attachment of ice dropped as the hydrophobic characteristics of the material soared. This was an additional discovery that they made [53]. Additionally, it was discovered by other researchers that in order to obtain a hydrophobic and, in actuality, an icephobic surface, it is necessary to produce surface roughness and low surface energy. An investigation of the effect that time has on the hydrophobicity of films that were formed on an aluminum substrate was carried out by G. Liu et al. The hydrophobic nature of the developed films resulted in a delay in the application of frosting and icing to surfaces that had been covered with metal oxide thin films. There was also a difference between coated and bare surfaces in terms of ice adhesion strength [54].

The thin film's optical characteristics, such as transmittance and absorbance spectrum, were determined with the assistance of a UV-Vis-NIR spectrophotometer. The transmission curves of thin film formed at different deposition powers of 200, 220, 240, and 260 W and at varied temperatures of 50, 100, 150, and $200\text{ }^{\circ}\text{C}$ are displayed in Figure 4a,b. The optical

transmittance of the film was measured in the span of 300 to 800 nm. The findings demonstrated that the transmission of films dropped as the depositing power and temperature increased. Furthermore, the transmittance was found to be in the range of 70 to 90% for both variations. In a 2016 study, Y. Xia et al. deposited AZO films at different power levels and found that when the power was increased, the crystal quality degraded and the film's transparency decreased [55]. S. Yang et al. (2019) examined how temperatures between 100 and 400 °C during deposition affected the optical properties of films. The transmittance of the thin films dropped from 91.3% to 88.4% as the synthesis temperature increased from 100 to 400 °C, with the greatest absorption observed in the 300–350 nm range [56]. Values have been shown to decrease as power and temperature increase, which has been documented by various researchers [57,58]. A coating's thickness and particle size determine its transmittance. Electron scattering impacts the transmission of light while operating at elevated powers and temperatures as a result of larger crystallite sizes and rougher surfaces.

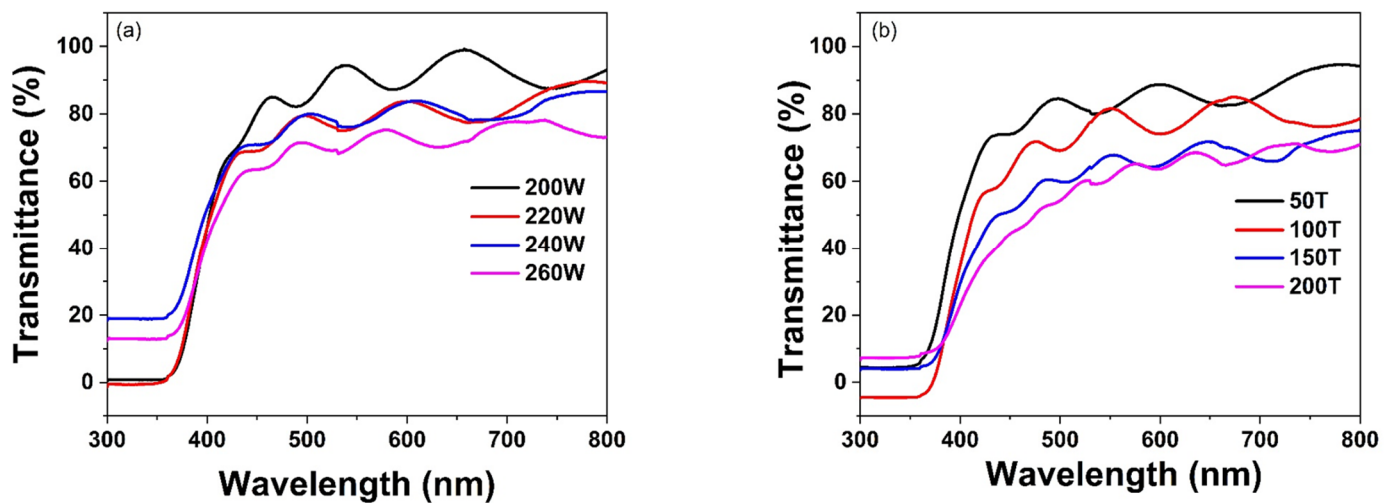


Figure 4. Optical transmittance curves for thin film of aluminum zinc oxide deposited at different (a) powers and (b) temperatures.

The film thickness was determined by using transmission data through the Swanepoel envelope technique [59]. It was noted that when the level of deposition power increased from 200 to 260 W, the film thickness also increased from 1079 to 1198 nm. A similar trend was seen while establishing a relation between deposition temperature and film thickness; as the temperature was elevated from 50 to 200 °C, the thickness values increased from 1207 to 1254 nm.

The value of refractive index 'n' for the sputtering power of 200 to 260 W is in the range of 1.49 to 1.51, while for deposition temperature from 50 to 200 °C, it varies from 1.50 to 1.52, which is mentioned in Table 3.

Table 3. Calculated parameters of AZO thin film.

Sample Name	RF Power (W)	Temperature (°C)	Gas Flow Rate of O ₂ /Ar (sccm)	Band Gap (eV)	Refractive Index (n)	Thickness (nm)
50 T	200	50	10:10	3.09	1.49	1207
100 T	200	100	10:10	3.00	1.50	1228
150 T	200	150	10:10	2.78	1.50	1232
200 T	200	200	10:10	2.61	1.51	1254
200 W	200	50	10:10	3.11	1.50	1079
220 W	220	50	10:10	3.01	1.50	1143
240 W	240	50	10:10	2.84	1.51	1150
260 W	260	50	10:10	2.80	1.52	1198

The measurement of the optical band gap for the thin film was performed using the absorption spectra of films, where absorption spectra were determined as a function of wavelength. With the help of the Tauc relation [59], optical band gap of the film was found from the absorption coefficient α . Figure 5 shows the plot of $(\alpha hv)^2$ on the vertical axis versus photon energy (hv) on the horizontal axis. The extrapolation of the linear region shows an approximation of the optical band gap. As shown in Figure 5a, band gap values range from 2.8 to 3.1 eV with variation in power from 200 to 260 W, whereas the value varies from 2.6 to 3.1 eV with variation in deposition temperature from 50 to 200 °C, as shown in Figure 5b. Alqahtani et al. developed single-layer (ZnO), bilayer (TiO₂ and WO₃/ZnO), and multilayer (WO₃/TiO₂/ZnO) thin films and observed that the band gap energy was in the range of 2.47 to 3.45 eV [60].

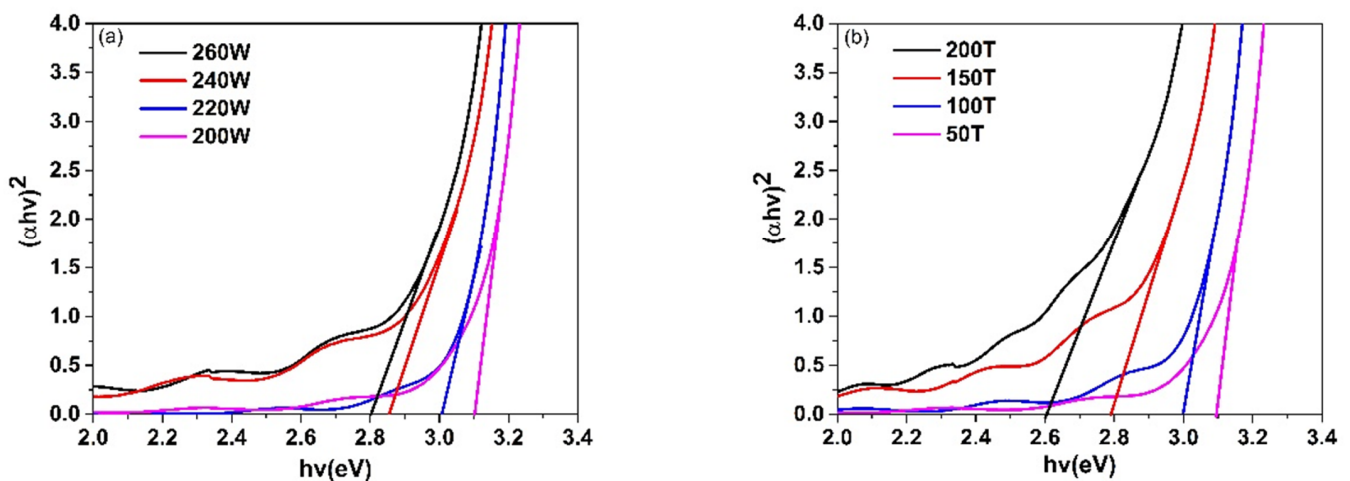


Figure 5. Optical absorption curves of aluminum zinc oxide thin film deposited at different (a) powers and (b) temperatures.

4. Conclusions

Using reactive magnetron sputtering, aluminum zinc oxide thin films were deposited at varying RF powers and temperatures. The (002) peak intensity increased with an increase in the deposition power and temperature. The maximum roughness of 54.6 nm and water contact angle of 110° were observed in AZO thin films at 50 °C and 260 W of RF power, and the surface energy was 17.09 mJ/m². These films have a good chance of being employed to make hydrophobic surfaces. The optical energy band gap narrows and the apparent refractive index rises when coating temperatures and powers are increased. The thin films of AZO exhibited a significant slowdown in the process of ice formation, with a lag measuring 3.38 times more than that which was found in the specimens that had not been treated. The findings and empirical data from this investigation indicate that hydrophobic surfaces that are produced using low-surface-energy materials and contain distinctive textures have a significant potential to serve as viable solutions for applications that need ice resistance. Increases in both temperature and power are likely the primary causes of the coatings' improved anti-icing properties. This research contributes to the advancement of the study of hydrophobicity and anti-icing attributes of AZO thin films. The purpose of this research is to boost both capabilities, which will allow the material to be used on surfaces for aviation windscreens, with the potential to improve the anti-icing attributes of the surface.

Author Contributions: S.R.: conceptualisation, methodology, software, validation, supervision. K.V.C.: formal analysis, investigation, data curation. N.P.P.: writing—original draft preparation, resources. V.V.: writing—review and editing. All authors have read and agreed to the published version of the manuscript.

Funding: This research received no external funding.

Institutional Review Board Statement: Not applicable.

Informed Consent Statement: Not applicable.

Data Availability Statement: All data is available within the manuscript.

Conflicts of Interest: The authors declare no conflicts of interest.

References

1. He, Z.; Ji, L.; Xing, Z. Experimental Investigation on the DLC Film Coating Technology in Scroll Compressors of Automobile Air Conditioning. *Energies* **2020**, *13*, 5103. [\[CrossRef\]](#)
2. Ogunlana, M.O.; Muchie, M.; Swanepoel, J.; Adenuga, O.T.; Oladijo, O.P. Numerical Modelling and Simulation for Sliding Wear Effect with Microstructural Evolution of Sputtered Titanium Carbide Thin Film on Metallic Materials. *Coatings* **2024**, *14*, 298. [\[CrossRef\]](#)
3. Prajapati, B.G.; Patel, P.; Patel, D. Mouth Dissolving Film as a Potential Dosage Form for Paediatric Usage. *J. Pharm. Biol. Sci.* **2024**, *11*, 133–141. [\[CrossRef\]](#)
4. Sevinç Özakar, R.; Özakar, E. Current Overview of Oral Thin Films. *Turk. J. Pharm. Sci.* **2021**, *18*, 111–121. [\[CrossRef\]](#)
5. Wang, K.; Shen, Y.; Duan, M.; Wu, T.; Zhao, J.; Wang, J. Non-Fluorinated Durable Water Repellent and Stain Resistant Coating. In Proceedings of the 3rd International Conference on Materials Chemistry and Environmental Engineering (CONF-MCEE 2023), Stanford, CA, USA, 18 March 2023. [\[CrossRef\]](#)
6. Zhu, Q.; Chua, M.H.; Ong, P.J.; Cheng Lee, J.J.; Le Osmund Chin, K.; Wang, S.; Kai, D.; Ji, R.; Kong, J.; Dong, Z.; et al. Recent Advances in Nanotechnology-Based Functional Coatings for the Built Environment. *Mater. Today Adv.* **2022**, *15*, 100270. [\[CrossRef\]](#)
7. Ben Chobba, M.; Weththimuni, M.L.; Messaoud, M.; Urzi, C.; Licchelli, M. Recent Advances in the Application of Metal Oxide Nanomaterials for the Conservation of Stone Artefacts, Ecotoxicological Impact and Preventive Measures. *Coatings* **2024**, *14*, 203. [\[CrossRef\]](#)
8. Khoo, Y.S.; Lau, W.J.; Liang, Y.Y.; Karaman, M.; Gürsoy, M.; Ismail, A.F. Eco-Friendly Surface Modification Approach to Develop Thin Film Nanocomposite Membrane with Improved Desalination and Antifouling Properties. *J. Adv. Res.* **2022**, *36*, 39–49. [\[CrossRef\]](#)
9. Fotovvati, B.; Namdari, N.; Dehghanghadikolaei, A. On Coating Techniques for Surface Protection: A Review. *J. Manuf. Mater. Process.* **2019**, *3*, 28. [\[CrossRef\]](#)
10. Piedade, A.P.; Pinho, A.C.; Branco, R.; Morais, P.V. Evaluation of Antimicrobial Activity of ZnO Based Nanocomposites for the Coating of Non-Critical Equipment in Medical-Care Facilities. *Appl. Surf. Sci.* **2020**, *513*, 145818. [\[CrossRef\]](#)
11. Patel, N.P.; Chauhan, K.V. Effects of Argon Partial Pressure Variations on Wettability and Anti-Icing Characteristics of Aluminum Doped ZnO Thin Films. *Mater. Res.* **2023**, *26*, e20220339. [\[CrossRef\]](#)
12. Baji, Z.; Pécz, B.; Fogarassy, Z.; Szabó, Z.; Cora, I. Atomic Layer Deposited Fe-Sulfide Layers with Pyrrhotite Structure Controlled by the Deposition Temperature. *Thin Solid Films* **2024**, *794*, 140267. [\[CrossRef\]](#)
13. Ivanova, T.; Harizanova, A.; Koutzarova, T.; Vertruyen, B.; Closset, R. Sol–Gel Synthesis of ZnO:Li Thin Films: Impact of Annealing on Structural and Optical Properties. *Crystals* **2024**, *14*, 6. [\[CrossRef\]](#)
14. Growth, J.; Wang, Z.; Liu, J.; Chen, P.; Liu, P.; Ma, J.; Xu, X.; Wei, Y.; Lebbou, K.; Xu, J. Growth and Characterization of Yb: CALYGLO Crystal for Ultrashort Pulse Laser Applications. *Crystals* **2024**, *14*, 120. [\[CrossRef\]](#)
15. Yue, F.; Zhu, J.; Geng, Y.; Xiang, M.; Zhu, Q. One-Step Synthesis of Single-Crystal Si₃N₄ Nanowires-Amorphous SiO₂ Beads Nanochains by Chemical Vapor Deposition. *Ceram. Int.* **2024**, *50*, 10635–10640. [\[CrossRef\]](#)
16. Nguyen, T.T.; Thai, T.T.; Paint, Y.; Trinh, A.T.; Olivier, M.G. Effect of Cerium Nitrate Concentration on Corrosion Protection of Hybrid Organic/Inorganic Si/Zr Sol-Gel Coating Applied on Hot-Dip Galvanized Steel. *Surf. Coat. Technol.* **2024**, *480*, 130562. [\[CrossRef\]](#)
17. Rawal, S.; Chauhan, K.V.; Patel, N.P. Characterization of Reactive Sputtered Chromium Oxynitride Coatings Developed on Glass Substrate. *Crystals* **2023**, *13*, 1262. [\[CrossRef\]](#)
18. Ellmer, K. Past Achievements and Future Challenges in the Development of Optically Transparent Electrodes. *Nat. Photonics* **2012**, *6*, 809–817. [\[CrossRef\]](#)
19. Bussell, B.C.; Gibson, P.N.; Lawton, J.; Couture, P.; Sharpe, M.K.; England, J.; Hinder, S.J.; Stolojan, V.; Thornley, S.A.; Baker, M.A. The Effect of RF Plasma Power on Remote Plasma Sputtered AZO Thin Films. *Surf. Coat. Technol.* **2022**, *442*, 128402. [\[CrossRef\]](#)
20. Ali, M.M.; Kabir, M.H.; Rahman, M.S. Exploration of Optical and Frequency Dependent Electrical Properties of Boron-Cobalt Co-Doped ZnO Thin Films. *Opt. Mater.* **2024**, *148*, 114949. [\[CrossRef\]](#)
21. Lekoui, F.; Amrani, R.; Hassani, S.; Garoudja, E.; Filali, W.; Ouchabane, M.; Hendaoui, N.; Oussalah, S. On the Substrate Heating Effects on Structural, Mechanical and Linear/Non-Linear Optical Properties of Ag–Mn Co-Doped ZnO Thin Films. *Opt. Mater.* **2024**, *150*, 115151. [\[CrossRef\]](#)
22. Tiwari, A.; Sahay, P.P. Improved Transparent Conductive Properties of Highly C-Axis Oriented ZnO Thin Films upon (Ga, Mg) Co-Doping. *Micro Nanostruct.* **2023**, *181*, 207617. [\[CrossRef\]](#)

23. De Oliveira, R.S.; Folli, H.A.; Stegemann, C.; Horta, I.M.; Damasceno, B.S.; Miyakawa, W.; Pereira, A.L.J.; Massi, M.; Da Silva Sobrinho, A.S.; Leite, D.M.G. Structural, Morphological, Vibrational and Optical Properties of GaN Films Grown by Reactive Sputtering: The Effect of RF Power at Low Working Pressure Limit. *Mater. Res.* **2022**, *25*, e20210432. [[CrossRef](#)]
24. Akmal, M.; Hatta, M.; Warikh, M.; Rashid, A.; Azlan, U.A.H.; Azmi, A.; Azam, M.A.; Moriga, T.; Pembuatan, F.K.; Jaya, H.T.; et al. Influence of Yttrium Dopant on the Structure and Electrical Conductivity of Potassium Sodium Niobate Thin Films. *Mater. Res.* **2016**, *19*, 1417–1422.
25. Oliveira, L.P.G.; Ribeiro, R.P.; Bortoleto, J.R.R.; Cruz, N.C.; Rangel, E.C. SiO_xC_yH_z-TiO₂ Nanocomposite Films Prepared by a Novel PECVD-Sputtering Process. *Mater. Res.* **2021**, *24*, e20210058. [[CrossRef](#)]
26. Li, J.; Lei, L.; Li, L.; Deng, B.; Zhao, G.; Jin, L.; Li, C. Microstructural Evolution and Its Influence on Oxygen Diffusion in Yttrium-Doped Ceria Thin Films. *Mater. Res. Express* **2022**, *9*, 046404. [[CrossRef](#)]
27. Bethge, O.; Nobile, M.; Abermann, S.; Glaser, M.; Bertagnolli, E. ALD Grown Bilayer Junction of ZnO:Al and Tunnel Oxide Barrier for SIS Solar Cell. *Sol. Energy Mater. Sol. Cells* **2013**, *117*, 178–182. [[CrossRef](#)]
28. Shen, H.L.; Zhang, H.; Lu, L.F.; Jiang, F.; Yang, C. Preparation and Properties of AZO Thin Films on Different Substrates. *Prog. Nat. Sci. Mater. Int.* **2010**, *20*, 44–48. [[CrossRef](#)]
29. Kim, D.S.; Park, J.H.; Lee, S.J.; Ahn, K.J.; Lee, M.S.; Ham, M.H.; Lee, W.; Myoung, J.M. Effects of Oxygen Concentration on the Properties of Al-Doped ZnO Transparent Conductive Films Deposited by Pulsed DC Magnetron Sputtering. *Mater. Sci. Semicond. Process.* **2013**, *16*, 997–1001. [[CrossRef](#)]
30. Yang, W.; Rossnagel, S.M.; Joo, J. The Effects of Impurity and Temperature for Transparent Conducting Oxide Properties of Al:ZnO Deposited by Dc Magnetron Sputtering. *Vacuum* **2012**, *86*, 1452–1457. [[CrossRef](#)]
31. Shu-wen, X. A Study of Annealing Time Effects on the Properties of Al:ZnO. *Phys. Procedia* **2012**, *25*, 345–349. [[CrossRef](#)]
32. Guo, T.; Dong, G.; Liu, Q.; Wang, M.; Wang, M.; Gao, F.; Chen, Q.; Yan, H.; Diao, X. Superlattices and Microstructures Optimization of Oxygen and Pressure of ZnO:Al Films Deposited on PMMA Substrates by Facing Target Sputtering. *Superlattices Microstruct.* **2013**, *64*, 552–562. [[CrossRef](#)]
33. Liu, G.; Yuan, Y.; Jiang, Z.; Youdong, J.; Liang, W. Anti-Frosting/ Anti-Icing Property of Nano-ZnO Superhydrophobic Surface on Al Alloy Prepared by Radio Frequency Magnetron Sputtering. *Mater. Res. Express* **2020**, *7*, 026401. [[CrossRef](#)]
34. Bai, Z.G.; Zhang, B. Fabrication of a Mechanically-Stable Anti-Icing Graphene Oxide-Diatomaceous Earth/Epoxy Coating. *Mater. Res. Express* **2019**, *6*, 085090. [[CrossRef](#)]
35. Farhadi, S.; Farzaneh, M.; Kulinich, S.A. Anti-Icing Performance of Superhydrophobic Surfaces. *Appl. Surf. Sci.* **2011**, *257*, 6264–6269. [[CrossRef](#)]
36. Chen, X.; Ma, R.; Zhou, H.; Zhou, X.; Che, L.; Yao, S.; Wang, Z. Activating the Microscale Edge Effect in a Hierarchical Surface for Frosting Suppression and Defrosting Promotion. *Sci. Rep.* **2013**, *3*, 2515. [[CrossRef](#)]
37. Chen, Y.; Chen, S.; Yu, F.; Sun, W.; Zhu, H.; Yin, Y. Fabrication and Anti-Corrosion Property of Superhydrophobic Hybrid Film on Copper Surface and Its Formation Mechanism. *Surf. Interface Anal.* **2009**, *41*, 872–877. [[CrossRef](#)]
38. Patel, N.P.; Chauhan, K.V. Effect of Sputtering Power and Substrate Temperature on Structural, Optical, Wettability and Anti-Icing Characteristics of Aluminium Doped Zinc Oxide. *Mater. Res. Express* **2022**, *9*, 076402. [[CrossRef](#)]
39. Misra, P.; Ganeshan, V.; Agrawal, N. Low Temperature Deposition of Highly Transparent and Conducting Al-Doped ZnO Films by RF Magnetron Sputtering. *J. Alloys Compd.* **2017**, *725*, 60–68. [[CrossRef](#)]
40. Tuyvaerts, R.; Raskin, J.P.; Proost, J. Opto-Electrical Properties and Internal Stress in Al:ZnO Thin Films Deposited by Direct Current Reactive Sputtering. *Thin Solid Films* **2020**, *695*, 137760. [[CrossRef](#)]
41. Cosme, I.; Vázquez-y-parraguirre, S.; Malik, O.; Mansurova, S.; Carlos, N.; Tavira-fuentes, A.; Ramirez, G.; Kudriavtsev, Y. Surface & Coatings Technology Differences between (103) and (002) X-Ray Diffraction Characteristics of Nanostructured AZO Films Deposited by RF Magnetron Sputtering. *Surf. Coat. Technol.* **2019**, *372*, 442–450. [[CrossRef](#)]
42. Li, W.; Hao, H. Effect of Substrate Temperature on High Rate Deposited ZnO:Al Films by Magnetron Sputtering. *Adv. Mater. Res.* **2012**, *432*, 480–483. [[CrossRef](#)]
43. Atilgan, A.; Ozel, K.; Sbeta, M.; Yildiz, A. Engineering the Visible Light Absorption of One-Dimensional Photonic Crystals Based on Multilayers of Al-Doped ZnO (AZO) Thin Films. *Mater. Sci. Semicond. Process.* **2023**, *166*. [[CrossRef](#)]
44. Aydin, H.; Aydin, C.; Al-Ghamdi, A.A.; Farooq, W.A.; Yakuphanoglu, F. Refractive Index Dispersion Properties of Cr-Doped ZnO Thin Films by Sol-Gel Spin Coating Method. *Optik* **2016**, *127*, 1879–1883. [[CrossRef](#)]
45. Wu, K.R.; Wang, J.J.; Liu, W.C.; Chen, Z.S.; Wu, J.K. Deposition of Graded TiO₂ Films Featured Both Hydrophobic and Photo-Induced Hydrophilic Properties. *Appl. Surf. Sci.* **2006**, *252*, 5829–5838. [[CrossRef](#)]
46. Cassie, A.B.D.; Baxter, S. Wetting of Porous Surfaces. *Trans. Faraday Soc.* **1944**, *40*, 546–551. [[CrossRef](#)]
47. Brassard, J.D.; Sarkar, D.K.; Perron, J. Studies of Drag on the Nanocomposite Superhydrophobic Surfaces. *Appl. Surf. Sci.* **2015**, *324*, 525–531. [[CrossRef](#)]
48. Gurav, A.B.; Lathe, S.S.; Vhatkar, R.S.; Lee, J.G.; Kim, D.Y.; Park, J.J.; Yoon, S.S. Superhydrophobic Surface Decorated with Vertical ZnO Nanorods Modified by Stearic Acid. *Ceram. Int.* **2014**, *40*, 7151–7160. [[CrossRef](#)]
49. Chang, C.J.; Kuo, E.H. Roughness-Enhanced Thermal-Responsive Surfaces by Surface-Initiated Polymerization of Polymer on Ordered ZnO Pore-Array Films. *Thin Solid Films* **2010**, *519*, 1755–1760. [[CrossRef](#)]
50. Patel, N.P.; Chauhan, K.V. Impact of Deposition Time and Working Pressure on Delay of Ice Formation on Aluminum Doped Zinc Oxide Thin Films. *Thin Solid Films* **2023**, *769*, 139750. [[CrossRef](#)]

51. Patel, N.P.; Chauhan, K.V. Consequences of Variation in Oxygen Partial Pressure on Zirconium Oxide Thin Films. *Mater. Today Proc.* **2022**, *62*, 3325–3329. [[CrossRef](#)]
52. Ahmad, D.; van den Boogaert, I.; Miller, J.; Presswell, R.; Jouhara, H. Hydrophilic and Hydrophobic Materials and Their Applications. *Energy Sources Part A Recovery Util. Environ. Eff.* **2018**, *40*, 2686–2725. [[CrossRef](#)]
53. Noormohammed, S.; Sarkar, D.K. Rf-sputtered Teflon®-modified Superhydrophobic Nanostructured Titanium Dioxide Coating on Aluminum Alloy for Icephobic Applications. *Coatings* **2021**, *11*, 432. [[CrossRef](#)]
54. Xia, Y.; Wang, P.; Shi, S.; Zhang, M.; He, G.; Lv, J.; Sun, Z. Deposition and Characterization of AZO Thin Films on Flexible Glass Substrates Using DC Magnetron Sputtering Technique. *Ceram. Int.* **2017**, *43*, 4536–4544. [[CrossRef](#)]
55. Yang, S.; Chen, F.; Shen, Q.; Zhang, L.; Huang, A.; Gu, H. Superior Crystallinity, Optical and Electrical Properties of Carbon Doped ZnO:Al Films at Low-Temperature Deposition. *Appl. Surf. Sci.* **2019**, *483*, 545–550. [[CrossRef](#)]
56. Patel, K.H.; Rawal, S.K. Influence of Power and Temperature on Properties of Sputtered AZO Films. *Thin Solid Films* **2016**, *620*, 182–187. [[CrossRef](#)]
57. Spadoni, A.; Addonizio, M.L. Effect of the RF Sputtering Power on Microstructural, Optical and Electrical Properties of Al Doped ZnO Thin Films. *Thin Solid Films* **2015**, *589*, 514–520. [[CrossRef](#)]
58. Patel, N.P.; Chauhan, K.V.; Desai, M.K. Effects of Power and Temperature on the Structural, Anti-Icing, Wettability, and Optical Properties of Zinc Oxide Thin Films. *Ceram. Int.* **2023**, *49*, 26943–26949. [[CrossRef](#)]
59. Ben Jbara, H.; Aubry, E.; Kanzari, M.; Billard, A.; Yazdi, M.A.P. Effect of Thermal Annealing on the Optoelectronic Properties of Cu-Fe-O Thin Films Deposited by Reactive Magnetron Co-Sputtering. *Thin Solid Films* **2021**, *721*, 138538. [[CrossRef](#)]
60. Alqahtani, A.; Alraddadi, S.; Alshomrany, A.S.; Qasem, A. Extended-Analysis for ZnO Monolayers, (TiO₂ & WO₃)/ZnO Bilayers, and WO₃/TiO₂/ZnO Multilayers Deposited on Silica Glass Substrates by RF Sputtering as Promising Cap Layers in Optoelectronic Applications. *Opt. Mater.* **2024**, *149*, 115002. [[CrossRef](#)]

Disclaimer/Publisher’s Note: The statements, opinions and data contained in all publications are solely those of the individual author(s) and contributor(s) and not of MDPI and/or the editor(s). MDPI and/or the editor(s) disclaim responsibility for any injury to people or property resulting from any ideas, methods, instructions or products referred to in the content.